JACS
JOURNAL OF THE AMERICAN CHEMICAL SOCIETY
Article
pubs.acs.org/JACS

Retinal Conformation Governs pK_a of Protonated Schiff Base in Rhodopsin Activation

Shengshuang Zhu,[†] Michael F. Brown,[‡,§] and Scott E. Feller*[,†]

[†]Department of Chemistry, Wabash College, Crawfordsville, Indiana 47933, United States
[‡]Department of Chemistry and Biochemistry and [§]Department of Physics, University of Arizona, Tucson, Arizona 85721, United States

Supporting Information

ABSTRACT: We have explored the relationship between conformational energetics and the protonation state of the Schiff base in retinal, the covalently bound ligand responsible for activating the G protein-coupled receptor rhodopsin, using quantum chemical calculations. Guided by experimental structural determinations and large-scale molecular simulations on this system, we examined rotation about each bond in the retinal polyene chain, for both the protonated and deprotonated states that represent the dark and photoactivated states, respectively. Particular attention was paid to the torsional degrees of freedom that determine the shape of the molecule, and hence its interactions with the protein binding pocket. While most torsional degrees of freedom in retinal are characterized by large energetic barriers that minimize structural fluctuations under physiological temperatures, the C6−C7 dihedral defining the relative orientation of the β-ionone ring to the polyene chain has both modest barrier heights and a torsional energy surface that changes dramatically with protonation of the Schiff base. This surprising coupling between conformational degrees of freedom and protonation state is further quantified by calculations of the pK_a as a function of the C6−C7 dihedral angle. Notably, pK_a shifts of greater than two units arise from torsional fluctuations observed in molecular dynamics simulations of the full ligand-protein-membrane system. It follows that fluctuations in the protonation state of the Schiff base occur prior to forming the activated MII state. These new results shed light on important mechanistic aspects of retinal conformational changes that are involved in the activation of rhodopsin in the visual process.

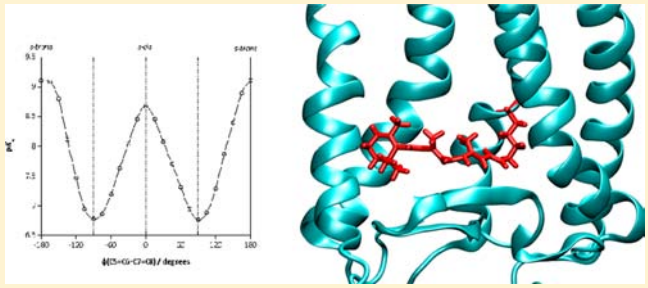

INTRODUCTION

Retinal-based proteins occurring in membranes are among the most ubiquitous proteins in the biosphere, accounting for the processes of solar energy transduction and ion transport in the case of microbial rhodopsins,[1,2] as well as signaling by visual pigments.[3−7] Rhodopsin is currently perhaps the best-studied system among the class of G protein-coupled receptors (GPCRs), which comprise the targets of about one-third of the pharmaceuticals in use today.[8−10] Upon photon absorption, the covalently bound ligand of rhodopsin, retinal, undergoes an 11-*cis* to all-*trans* isomerization, culminating in a series of photoproducts and subsequent G protein activation. The activation mechanisms for GPCRs are clearly of great significance, both as fundamental cellular processes and as important targets for pharmacological intervention (see, for example, refs 11−15).

Our understanding of the rhodopsin activation process relies heavily on structural models from X-ray crystallography that describe the conformations of both the dark state[16,17] and the metarhodopsin II (MII)-like activated state[18,19] that binds the G protein transducin, as well as the ligand-free opsin state.[20] In the case of the prototypical GPCR rhodopsin, numerous experimental studies have examined structural,[21−26] dynamic,[27−31] and spectroscopic[32−34] features of both the ground state, that is, dark state, and the activated states in the photoinitiated process that begins the visual cascade. Unusual features of rhodopsin, compared to other ligand-activated GPCRs, include the nature of its ligand, which is covalently bound to the protein (opsin), and the mechanism by which the activation process is initiated, that is, the absorption of a photon of light. The conformation of the ligand, retinal, is intimately coupled to the receptor state, undergoing a conformational change, for example, *cis* to *trans* isomerization of the C11═C12 bond in the photoconversion from the dark state. Adiabatic thermal relaxations lead to the metarhodopsin I (MI) intermediate, followed by a change in protonation, for example, the deprotonation of the protonated Schiff base upon formation of the MII activated state. Nonetheless, there remain many critical details of the intermediate processes to be elucidated, such as the structural details of the MI intermediate and the crucial deprotonation of the Schiff base required for MII formation.[22,26,35]

Received: January 10, 2013
Published: May 23, 2013

   dx.doi.org/10.1021/ja4002986 | J. Am. Chem. Soc. 2013, 135, 9391−9398

Augmenting the body of experimental work on rhodopsin and retinal are numerous computational studies—ranging from quantum mechanical descriptions of the electronic properties of retinal,[36−41] to classical molecular dynamics (MD) studies of the entire protein system embedded in a phospholipid bilayer membrane.[42−52] Additional studies have examined the related system bacteriorhodopsin, a light harvesting proton pump that also employs a covalently bound retinal cofactor.[53−56] Indeed, MD simulations of rhodopsin have been an especially active area of computational research over the past decade, following initial publication of its X-ray crystallographic structure,[57] the first GPCR to have its structure determined.[16,17] To date, simulations have examined the dark state of rhodopsin,[43,44,47,51] as well as initial states along the activation pathway up to the MI state[50,58,59] and even the MII state.[60] Rapidly increasing computational power—provided by parallelization, coarse-graining,[61−67] and especially by special-purpose computers optimized for MD simulations[68]—has opened up the possibility of accessing longer time-scale processes, such as those underlying the formation of the MII state of rhodopsin. These efforts are supported by new X-ray structures that capture activated state conformations of GPCRs[15,18,19,69] and are pertinent to experiments indicating that an ensemble of conformations characterizes the activated state.[22,26,35,70] A significant challenge to the implementation of MD simulations of the MII state is the change in protonation state of key amino acids in the protein, as well as the deprotonation of the retinal protonated Schiff base.[22,26,58]

The retinal moiety is a particularly challenging target for molecular mechanics (MM)-based simulation approaches. For example, we recently showed that each retinal methyl substituent must be considered individually in the MM force field, as the methyl rotation barriers depend sensitively on the topology and protonation state of the Schiff base.[71] In our previous MD calculations,[59] we had been unable to reproduce the behavior of the retinal methyl groups seen experimentally with solid-state NMR spectroscopy,[25,29] which provides an important new source of data to validate the retinal force field. However, using larger model compounds and/or higher levels of theory than previous studies,[42,72−74] we were able to reproduce the experimentally observed trends in methyl rotation barriers. The observation that protonation effects on polyene chain conjugation extend through the molecule, and significantly even to the retinylidene methyl groups,[71] motivated us to revisit the retinal force field by conducting high-level electronic structure calculations on the entire retinal moiety. In this article we report a number of significant new findings pertinent both to the quantum chemical basis of retinal dynamics, in particular the role of the orientation of the β-ionone ring in the deprotonation process, as well as the use of MD calculations as a vehicle for integrating experimental measurements spanning a range of time scales.[13,21−23,26,29,35]

METHODS

Ab initio Quantum Chemical Calculations. Quantum chemical calculations were performed with the GAUSSIAN 09 program to default tolerances using multicore AMD processors. Optimized geometries were obtained for both the *trans* and *cis* conformations of each polyene chain torsion angle for the model compounds in Figure 1. In these retinal analogues, a methyl amino group has replaced the Lysine side chain that provides the linkage to the protein in rhodopsin. The compounds studied were, namely, *N*-(all-*trans*-12-*s*-*cis*-retinylidene)-*N*-methyliminium having a protonated Schiff base (PSB) (Figure 1, top), and *N*-(all-*trans*-12-*s*-*cis*-retinylidene)-*N*-methylimine with a deprotonated Schiff base (SB) (Figure 1, bottom). Dihedral coordinate scans were performed at the second-order Møller−Plesset (MP2) level of theory with a 6-31G* basis set. To reduce computational time, a semirelaxed dihedral scan strategy was employed for torsions along the main chain, whereby the two dihedrals adjacent to the scanned dihedral were free to rotate while other polyene torsions were fixed in the *trans* conformation. All β-ionone ring torsions, all methyl torsions, as well as the C6−C7 torsion were given complete freedom in every scan. Scans used increments of 15° for each step, covering the entire range, that is, −180° and 180°. All scans were begun from the *cis* conformation and convergence was tested by comparing the end of the scans, that is, −180° and 180°, to the *trans* optimized results. The choices of theory level and basis set were based on our previous experience parametrizing singly and doubly bonded hydrocarbon chains for saturated, monounsaturated, and polyunsaturated fatty acids.[75] While the calculation of torsional barriers for rotation about double bonds can be challenging using single configuration methods, the precise values of these barriers are not critical for MD simulations under physiological conditions where such states are not energetically accessible.

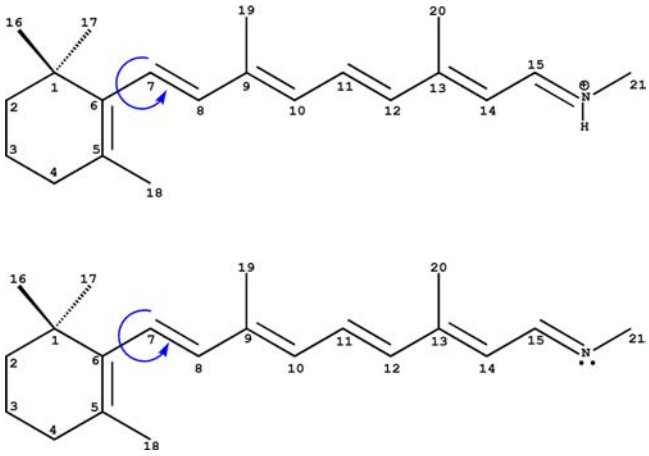

Figure 1. Structures and naming schemes for the model compounds used in this work. (top) Protonated Schiff base (PSB) model compound *N*-(all-*trans*-12-*s*-*cis*-retinylidene)-*N*-methyliminium, and (bottom) deprotonated Schiff base (SB) model compound *N*-(all-*trans*-12-*s*-*cis*-retinylidene)-N-methylimine. The blue arrow indicates the torsional rotation that defines the orientation of the β-ionone ring to the polyene chain.

Molecular Mechanics Calculations. Molecular mechanics optimizations were performed with CHARMM.[76] Since the primary focus of this study was to refine the polyene chain torsional potentials while maintaining consistency with the CHARMM protein, lipid, and water force fields, we adopted previously developed force field parameters for terms other than the torsional potential. For neutral retinal, all parameters for the β-ionone ring as well as all parameters excluding torsions for the polyene chain and deprotonated Schiff base were taken from the CHARMM General Force Field.[77] For protonated retinal, β-ionone ring parameters were identical to neutral retinal, while for the polyene chain and PSB the internal energy parameters and atomic charges are unique to each atom, due to the delocalization of the positive charge. For these atoms we employed the parameters developed by Nina et al[78] that used the CHARMM force field development strategy. For both neutral and protonated retinal, we found the QM minimized energy structure was reproduced with good accuracy by the MM force field. The entire retinal force field (neutral and protonated) is included in the Supporting Information (SI).

To determine dihedral parameters, coordinate scans were carried out in CHARMM, which paralleled the QM calculations. Beginning from C5═C6−C7═C8 along the main chain each dihedral angle was examined sequentially. For the dihedral angle of interest the force constant(s) were set to zero, and the difference between the QM

dx.doi.org/10.1021/ja4002986 | J. Am. Chem. Soc. 2013, 135, 9391−9398

results and the remaining terms in the potential energy function were fit by adjustment of the force constant of each dihedral, fold number, and phase angle. A second stage of refinement was to rescan each dihedral angle using the new parameters for the other dihedrals. All of the dihedrals showed consistent results with the exception of C5═C6−C7═C8. This is because C5═C6−C7═C8 rotation involves strong steric interactions between the β-ionone ring and the polyene chain, making the C5═C6−C7═C8 and C6−C7═C8−C9 torsional parameters highly dependent on each other. Thus, C5═C6−C7═C8 and C6−C7═C8−C9 dihedrals were repeatedly parametrized until the results converged with the *ab initio* calculations.

pK_a Calculations. In this work, the pK_a as a function of the C1−C6−C7═C8 dihedral angle was calculated using a thermodynamic cycle as described by Shields and co-workers.[79] Briefly, the connection between the pK_a value and the energy states of the protonated and deprotonated species is $\Delta G^\circ = -RT\ln K_a$. Computationally, we can calculate the free energy of deprotonation by calculating ΔG° in a cycle, where the enthalpy of deprotonation is computed in the gas phase, and the solvation free energy of each species, ΔG_{sol}, is computed quantum mechanically using an implicit solvent. The major contributor to the enthalpy of deprotonation (and the only term that is a function of torsion angle based on our calculations) is the so-called proton affinity (PA), defined as the difference between the absolute energies of the deprotonated and protonated molecule species, PA = E(SB) − E(PSB). At a temperature of 25 °C, this simplifies to pK_a = [PA + ΔG_{sol}(SB) − ΔG_{sol}(PSB) − 270.28567]/1.36449 where ΔG_{sol} was calculated with the SM8 solvent model and energies are in units of kcal/mol.[80]

RESULTS

Bond Orders and Torsional Barriers Manifest Retinal Charge Delocalization. The lowest energy conformation of protonated retinal in the model compound (Figure 1) showed all the features typical of previous computational and experimental investigations of related compounds. For example, the partial delocalization of the positive charge of the PSB along the polyene chain manifests itself in the calculated carbon−carbon and carbon−nitrogen bond lengths. Figure 2A presents all heavy atom bond lengths in the retinylidene model compound for both the protonated and deprotonated states. While the neutral (deprotonated) species exhibits localized bonds along the polyene chain, with a repeated pattern of shorter (double) bonds of ∼1.37 Å and longer (single) bonds of ∼1.45 Å, the positively charged species shows significant resonance effects with intermediate length bond lengths near the PSB due to noninteger bond orders. The effect declines with distance from the Schiff base, with the protonated C6−C7 bond length within ∼1% of the corresponding bond in the deprotonated molecule. The extensive changes in electronic structure upon protonation/deprotonation also have a large effect on torsional barriers along the polyene chain (Figure 2B). The larger (∼35 kcal/mol) and smaller (∼8 kcal/mol) barriers for rotation about double and single bonds, respectively, in the neutral molecule contrast with the intermediate rotation barriers seen in the protonated species. Again, the polyene segments near the β-ionone ring appear to show little effect of protonation.

Torsional Energies of Retinal Depend on Protonation State of Schiff Base. Figure 3 shows the torsional energy profiles for selected bonds in detail. The C14−C15 dihedral, near the Schiff base, serves as an example of an energy surface that changes dramatically upon protonation, while the C7═C8 torsion nearer the β-ionone ring shows a small relative difference in barrier height with protonation state. In both cases, the likely effect on polyene chain conformation is

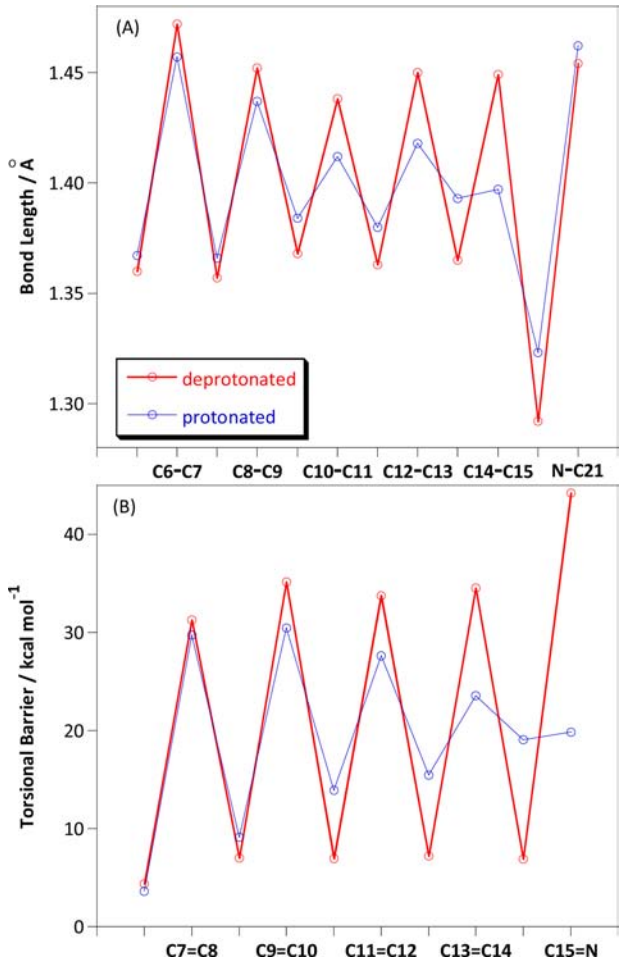

Figure 2. Bond lengths and torsional barriers of polyene chain in retinylidene model compounds depend on protonation state of Schiff base. (A) Polyene chain bond lengths in the energy-minimized conformations of the charged (blue) and neutral (red) model compounds. (B) Polyene chain torsional barriers for the charged (blue) and neutral (red) model compounds. While clear alternation between single and double bonds is observed in the deprotonated species, intermediate bond length and torsional barriers are seen in the protonated species.

minimal, because the rotational barriers remain thermally inaccessible under physiological conditions for both protonated and neutral species. Figures 2 and 3 both suggest that the energy landscapes of the two species are converging as the β-ionone ring is approached. It is surprising, therefore, that the torsional energetics of the C6−C7 torsion—defining the orientation of the ring with respect to the polyene chain—is strongly affected by protonation with the torsional profile exhibiting changes in both shape and magnitude. Specifically, Figure 4 shows that the protonated species has lower rotational energy barriers as well as an additional low energy conformation (ϕ = ∼180°, that is, *s-trans*) that does not exist in the deprotonated molecule. This result is especially surprising given the distance between the PSB and β-ionone ring, and the apparent convergence of the protonated and deprotonated model compounds for bond lengths (Figure 2A), polyene chain rotation barriers (Figure 2B), and methyl substituent rotation barriers,[71] in the vicinity of the β-ionone ring. The observation of a lower torsional barrier for the protonated species is counterintuitive in that protonation is

dx.doi.org/10.1021/ja4002986 | J. Am. Chem. Soc. 2013, 135, 9391−9398

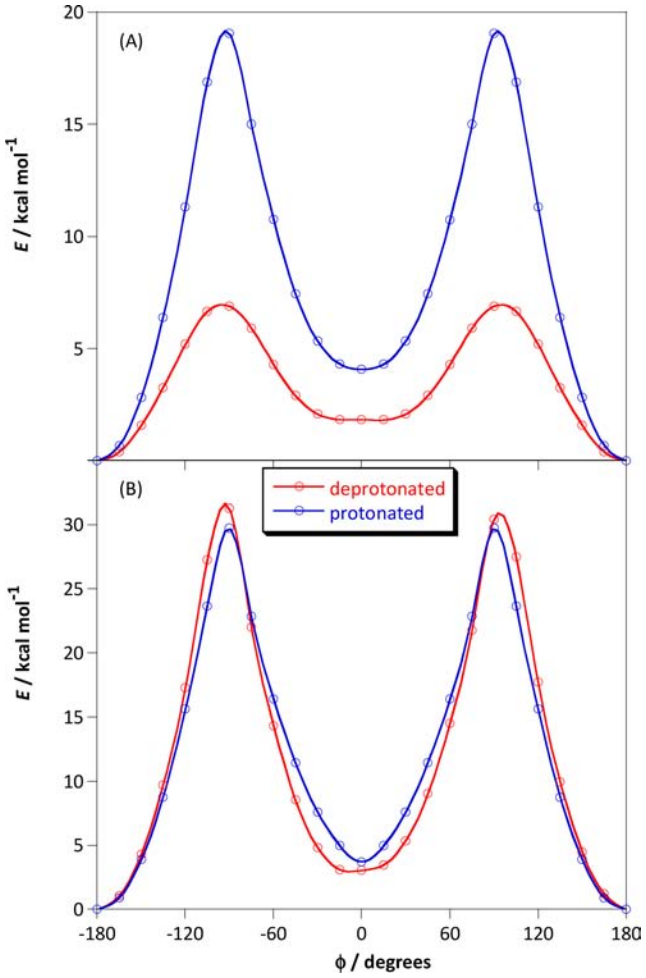

Figure 3. Torsional barriers depend on position of bond within the retinal polyene chain. Representative torsional energy profiles for dihedral rotation about bonds at opposite ends of π-conjugated system of retinylidene moiety: (A) C13═C14−C15═N and (B) C6−C7═C8−C9 polyene dihedrals. The protonated species results are given in blue while the neutral species results are shown in red. While the protonated and deprotonated species give similar results for bonds near the β-ionone ring, significant differences are observed near the PSB.

expected to lead to charge delocalization and the development of partial double bond character, and hence a larger barrier to rotation, in the C6−C7 bond. This result, however, can be understood after considering the unusual torsional energy surface for C6−C7. While the other conjugated polyene segments have energy minima at *cis* and *trans*, and hence barriers at ±90°, the C6−C7 torsion has a barrier at *s-cis*. Examination of Figure 4 shows the expected destabilization of the protonated species at ±90° (and hence stabilization of *s-cis*), consistent with increasing double bond character.

Retinal Conformation and Schiff Base Protonation State Exert Mutual Effects upon One Another. While the preceding discussion has considered the effect of deprotonation on conformational energetics, an alternative is to think about the effect of conformation on the energetics of deprotonation. Tajkhorshid and co-workers[73,74] have examined this aspect for various retinal analogues using quantum chemical methods, specifically density functional theory (DFT), to compute the proton affinity as a function of changes in molecular conformation and structure. For example, they observed that

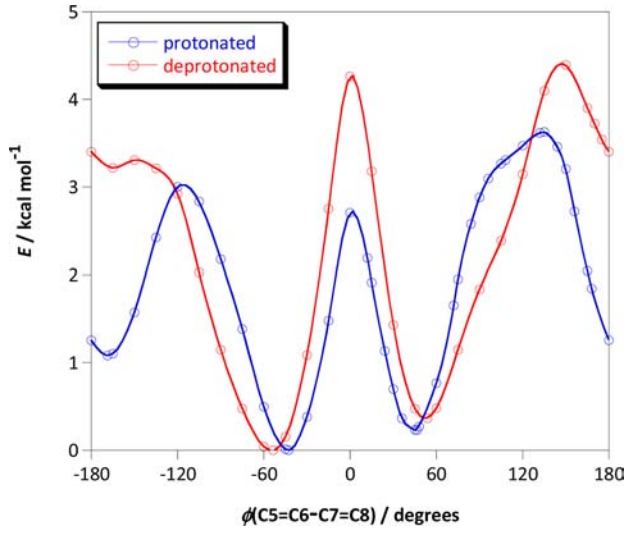

Figure 4. Torsional barriers of β-ionone ring are less than for polyene chain and depend on protonation state of Schiff base at opposite end of retinal. The torsional energy profile is shown for the C5═C6−C7═C8 dihedral that describes the orientation of the β-ionone ring to the polyene chain (see Figure 1). Results for the protonated species are given in blue while the neutral species results are shown in red.

PA increased when double bonds are rotated away from their minimum energy conformations. On the other hand, single bond rotation caused PA to decrease. In addition, they found that addition of methyl groups to the model molecule decreased the energy barrier of bond rotation due to their steric effect, whereas the electron-donating effect of a methyl group increased the PA of retinal. While these earlier calculations are instructive in demonstrating the relationship between conformation and protonation state, the large rotational barriers for polyene chain torsions (see Figure 3), combined with the relatively tight packing within the retinal binding pocket, limits conformational flexibility of the polyene chain. Sampling the conformational space where large changes in proton affinities were observed in the published studies, for example, ±90°, are thus prohibited. By contrast, Figure 4 shows that the C6−C7 torsion has low energy barriers, particularly in the protonated ground state. While the results in Figure 4 are for a model compound in the gas phase, a study combining atomistic MD simulation with ^{2}H solid state NMR showed significant flexibility of the C6−C7 torsion with isomerization on the 100-ns time scale.[59]

To directly connect the calculated energy surfaces to observables, we computed the pK_a of the protonated model compound as a function of the C6−C7 torsion, and have plotted the results in Figure 5. The important feature is the dramatic difference in pK_a between the conformer in the *s-trans* state (~180°) versus the two twisted *s-cis* conformers (±50°). Remarkably, while the conformational energy of these states differs by only approximately 1 kcal/mol, a striking two-unit shift in pK_a is observed, corresponding to a 100-fold change in the equilibrium constant. Importantly, the barrier to interconversion among these two states is thermally accessible under physiological conditions, which contrasts with the remaining polyene chain torsions, whose barriers to rotation are much higher. To explore the effect of the level of quantum chemical theory, we repeated the torsional energy profile and pK_a calculations at lower levels of theory (Hartree−Fock and DFT). We found that while all three methods produced

dx.doi.org/10.1021/ja4002986 | J. Am. Chem. Soc. 2013, 135, 9391−9398

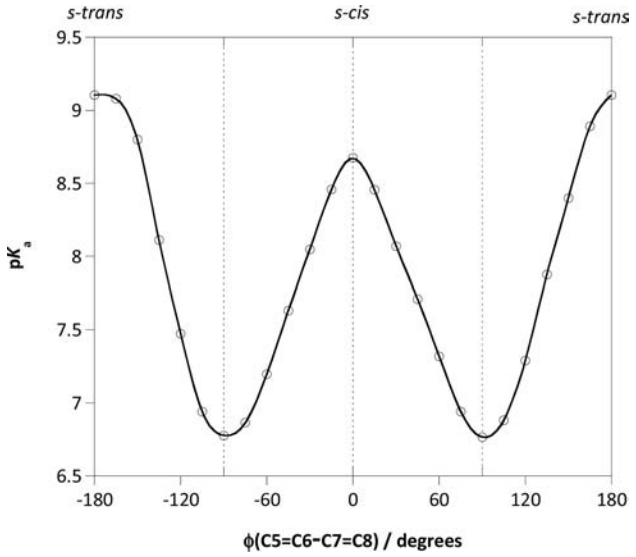

Figure 5. Protonation state of Schiff base and conformational energetics of β-ionone ring of retinal are mutually interdependent. The value of the pK_a of the retinylidene Schiff base is shown as a function of the C5═C6−C7═C8 dihedral that defines the orientation of the β-ionone ring to the polyene chain (see Figure 1). Planar conformations (ϕ = 0, 180°) favor the protonated form, that is, making it a weaker acid, while deviations in planarity correspond to lower pK_a values and hence a more acidic species.

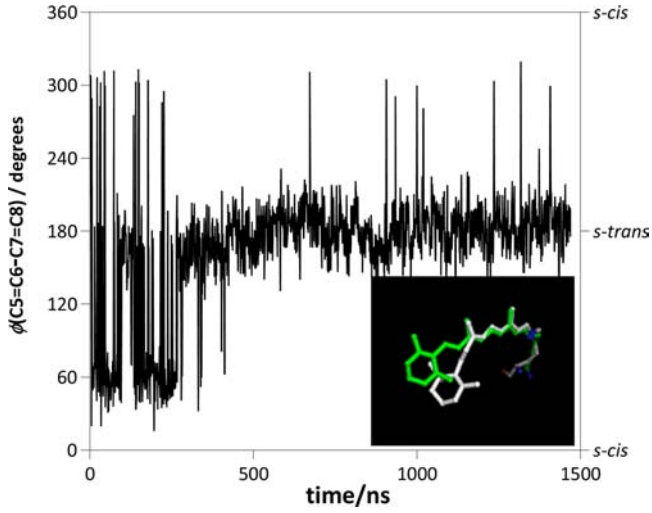

Figure 6. Molecular simulations of rhodopsin in explicit bilayer membrane show the torsional angle defining the β-ionone ring fluctuates between positively and negatively twisted *s-cis* conformations. A dominant population of *s-trans* is found for the MI photoproduct at longer time intervals. The C5═C6−C7═C8 dihedral angle is shown as a function of time after isomerization of the C11═C12 torsion, observed in a molecular dynamics simulation of rhodopsin in an explicit membrane. The dihedral data were taken from previously published simulations reported in ref 82. (Inset) Molecular graphics of the retinal near the beginning of the simulation (gray) and near the end of the simulation (green) after aligning the structures.

qualitatively similar pK_a shifts as a function of torsion angle, only the higher level MP2 computations reproduced the experimentally measured pK_a of the retinal Schiff base of 7.4 ± 0.1.[81]

Conformational Dependence of pK_a Values for Retinal Schiff Base. For the conformational dependence of pK_a shown in Figure 5 to be relevant for the rhodopsin activation mechanism, one would need conformational transitions between states having different pK_a values. The two-way protein-induced ligand conformational changes could move the retinal from a state that favors protonation to one that favors deprotonation via rotation of the β-ionone ring. From the standpoint of the β-ionone ring the pK_a of the PSB depends on its conformation; and conversely from the view of the pK_a (if it had one) the β-ionone ring conformation depends on whether it is protonated or deprotonated. To examine the conformational states of retinal during the activation process, we computed the time series for the C5═C6−C7═C8 dihedral angle following isomerization of the C11═C12 bond, which is rotated upon photon adsorption, from a previously published 1.5 μs MD simulation of rhodopsin in an explicit lipid membrane.[82] (Details of the simulation are found in this reference.) The force field for the simulation had a C6−C7 rotation barrier that is similar to what was computed in the present work, and thus provides insight into the degree of β-ionone ring mobility that might be expected within the rhodopsin binding pocket. Upon isomerization of the C11═C12 double bond, the C6−C7 torsion undergoes rapid conformational changes, moving between the twisted *s-cis* conformations (±50°) and the *s-trans* conformation (180°) for several hundred nanoseconds (Figure 6). At longer times, the retinal ligand settles into a predominantly *s-trans* state that is stable on the μs time scale accessible to the simulation. Importantly, this *s-trans* conformation stabilizes the protonated state, potentially maintaining the PSB until additional conformational rearrangements of the protein have taken place. The simulation also shows that conformational flexibility is retained by the ligand, though fluctuations occur on a much longer time scale of approximately once per 100 ns. It is noteworthy that these fluctuations rotate the C6−C7 torsion from an *s-trans* to a twisted *s-cis* conformation, which corresponds to movement from the maximum pK_a to near the minimum pK_a, that is, conformational fluctuations observed in the simulation lead to shifts of greater than two pK_a units.

DISCUSSION

Changes in both structure and dynamics underlie the reaction coordinates for GPCRs such as rhodopsin,[18,19] the β-adrenergic receptors,[83−86] and other GPCRs of remarkable significance to human biology.[15,87,88] For rhodopsin, the role of dynamics in its activation mechanism has been explored both through experimental[28,29,33,34] and theoretical[47,50] approaches. Activation by light entails ultrafast photoisomerization of retinal, whereby coherent wave packet dynamics on the excited state potential surface occur nonadiabatically through a conical intersection with the ground state potential surface of the photoproduct.[33,34,38] The impulsive nuclear response explains the ultrafast isomerization,[34] which is followed by a series of adiabatic thermal relaxations, culminating in the MI−MII equilibrium and guanine nucleotide exchange on the G protein transducin.[4,89] The fluctuating equilibrium between MI and MII states entails large-scale restructuring of transmembrane helices H5 and H6, as first revealed by the site-directed spin-labeling studies of Hubbell and co-workers,[21,90] and later confirmed by X-ray crystallography.[18−20] The following question thus arises: how are the large-scale structural rearrangements initiated by changes in the local dynamics of the retinylidene ligand of rhodopsin? Moreover, are changes in

dx.doi.org/10.1021/ja4002986 | J. Am. Chem. Soc. 2013, 135, 9391−9398

the local pK_a values of the retinylidene Schiff base involved? Here, the confluence of molecular simulations with spectroscopic studies has much to offer, and rests upon a firm quantum mechanical treatment of the retinal chromophore and the changes undergone upon photoactivation.

Molecular Simulations Depend on Retinal Electronic Structure and Are Influenced by Charge Delocalization. A notable challenge for molecular simulations of retinal proteins is the very different electronic structures of the protonated and neutral SB species. In protonated retinal, the conjugated polyene chain allows delocalization of the positive charge across the molecule, and hence stabilizing the PSB (see Figure 3 of ref 91 for enumeration of the various resonance forms). Charge delocalization, however, is not uniform along the chain, because the more electropositive nitrogen atom yields a greater propensity for positive charge near the PSB. This electronic effect leads to bond lengths near the PSB that are nearly equivalent, that is, the formal single and double bonds show similar lengths, while those near the β-ionone ring show the expected bond length alternation. While molecular mechanics force fields describing this effect as well as the remaining internal degrees of freedom in protonated retinal[92] have been developed and tested in large-scale MD simulations, less attention has been given to comparison with the deprotonated state force field, with the exception of methyl group energetics in ref 71.

We note that the tetra-substituted C5=C6 double bond of retinal is electron rich, and thus can have a substantial effect on conjugation involving the entire π system. The protonated form becomes more acidic when the C6−C7 dihedral is perpendicular to the rest of the polyene plane, due to a reduction of electron density and less charge delocalization of the iminium salt. Remarkably, this effect is transmitted through nine chemical bonds. Although an increase in pK_a with decreasing conjugation is expected, an increase of more than two pK_a units is rather surprising. It is worth noting that our proton affinity calculations correspond to the gas phase, and the pK_a computation employs an implicit solvent to represent an aqueous medium, neither of which fully captures the complex environment of the rhodopsin binding pocket. The retinal binding pocket of rhodopsin is inaccessible to water in the dark state (as judged by hydroxylamine reactivity[93]) but becomes at least partially hydrated in the MI state.[94] Additionally, motions of the protein during activation involves reorganization of charged groups near to the PSB, for example, the complex counterion involving the carboxylates Glu^{113} and Glu^{181}.[82] While changes in interactions with water and proteins during photoactivation clearly have the potential to alter the pK_a of the PSB, these effects should be considered as additional to those arising from ligand electronic structure.

Retinal Conformation and Schiff Base Protonation State Exert Mutual Effects upon One Another. Complicating the analysis of PSB deprotonation are the numerous factors affecting the acidity of the PSB, as well as the manner in which they change as a function of time during the photoactivation process. The protein, for example, has a large effect on the pK_a of the retinal Schiff base, as evidenced by the measured pK_a rising from 7.4 as a free ligand in aqueous ethanol solution to 14.5 in the case of bacteriorhodopsin.[81] Another potential mechanism for modifying the acidity of the PSB is coupling of the conformational change within retinal to deprotonation. This will be the case whenever the energy surface of a conformational degree of freedom, for example rotation of a torsion angle, is modified upon deprotonation. Essentially, whenever conformational energetics depend on protonation state, then the energetics of deprotonation will depend explicitly on conformation. Previously, Tajkhorshid and co-workers[74] studied this effect using quantum chemical calculations of various model compounds to represent the retinal PSB. They computed the proton affinity of numerous model compounds with structures mimicking the retinal molecule polyene chain. The effect of conformation was examined by comparing proton affinities of the all-*trans* chain with those computed after rotating the various torsion angles by 90°. They observed that rotation about double bonds increased PA, that is, decreased acidity of the PSB, while rotation about single bonds had the opposite effect. Additionally, they found that the location of methyl groups on the chain alters the PA and its dependence on conformation, such that rotation about specific bonds can maximally affect the pK_a value. The key result of the present work is that the orientation of the β-ionone ring can serve as a switch between conformations that differ by greater than two pK_a units, and importantly these conformations are thermally accessible under physiological conditions.

Crystallographic Structures and Molecular Dynamics Simulations of Rhodopsin Reveal Changes in the β-Ionone Ring Due to Isomerization of the Polyene Chain. The recently published crystallographic structures of an activated MII-like conformation of rhodopsin reveals two separate conformational changes of the retinal ligand within the binding cavity.[14,18,19] As expected, the polyene C11=C12 dihedral moves from *cis* (dark state) to *trans* (MII). However, an additional rotation is also observed around the C6−C7 bond of the β-ionone ring, which changes from ∼−50° (average of the dark state structures) to ∼+50° in the MII structures, notably accompanied by a long-axis rotation of the entire retinal molecule.[18] This raises the obvious question as to the path of this transition: namely, does the β-ionone ring rotate through an *s-cis* (0°) or *s-trans* (180°) intermediate during the photoactivation process? The calculated C6−C7 energy surface (Figure 4) is ambiguous on this point. No matter if the isomerization occurs pre- or postdeprotonation, the barrier to rotation through *s-cis* is similar to the rotational barrier through *s-trans*. It is, however, possible that interactions between the ligand and the protein alter the effective barriers to favor one path over the other. The MD simulation results in Figure 6 support this idea, with many observed transitions between −60° and +60° through *s-trans* shortly (<200 ns) after isomerization of the C11=C12 torsion angle. Additionally, the MD trajectory clearly settles into the *s-trans* state on the μs time scale. It is noteworthy that the distribution of retinal conformers observed in the latter part of the simulation reproduces experimental solid-state ^{2}H NMR spectra for the retinal methyl groups, including the C5 methyl group which is sensitive to the β-ionone ring conformation.[58] The NMR results correspond to the MI conformation, suggesting that the state of the C6−C7 torsion angle may be *s-trans* in the preactivated MI intermediate.

Potentially arguing against the path through *s-trans* are the X-ray structures of the short-time intermediates bathorhodopsin and lumirhodopsin,[95,96] which give C6−C7 dihedral angles of −14° and −5°, respectively. The low rotational barriers of the protonated retinal (Figure 4) and the high mobility observed in the simulation during the period immediately following isomerization (Figure 6), however, are consistent with a highly

dx.doi.org/10.1021/ja4002986 | J. Am. Chem. Soc. 2013, 135, 9391−9398

dynamic β-ionone ring. Presumably, it could adopt numerous conformations during these short-lifetime intermediate states, before stabilizing in an *s-trans* configuration, corresponding to the longer-lived MI state. Further support for an *s-trans* C6−C7 dihedral in the MI state of rhodopsin is found from a survey of retinal conformations in the X-ray structures in the protein data bank (PDB). If such a survey is broadened to include nonvisual rhodopsins, there are many examples of all-*trans* polyene chains (with protonated Schiff bases) that show the C6−C7 torsion in the *s-trans* conformation. These include the many bacteriorhodopsin ground-state structures, as well as examples from archaerhodopsin, sensory rhodopsin, halorhodopsin, and xanthorhodopsin.[97] Thus, both the MD analysis (validated by ^{2}H NMR) and the conformational preference observed in the PDB support an all-*trans* configuration of retinal in MI that includes a coplanar orientation of the β-ionone ring and the polyene chain arising from a *trans* C6−C7 torsion angle.

CONCLUSIONS

Our quantum chemical calculations suggest a surprising mechanism in which remote control of the PSB is achieved by the motion of the β-ionone ring despite their separation by nine chemical bonds. The observation that the pK_a of the protonated Schiff base is a function of β-ionone ring orientation has implications for the rhodopsin activation process, whereby the MI intermediate includes a planar retinal that favors the protonated form, that is, higher pK_a value. The intrinsic conformational freedom of the β-ionone ring in the protonated form of the ligand could be modified by the protein to maintain the *trans* conformation in MI, until the stage in the activation process where deprotonation of the PSB is required. At that point a protein conformational change could allow rotation of the β-ionone ring into a nonplanar conformation that favors the deprotonated state. Once deprotonation had occurred the much higher energy barrier for β-ionone rotation of the neutral species would ensure the ligand stays locked in a fixed conformation. In this way the activated MII state is stabilized leading to the resultant visual signaling via binding of the G-protein transducin.

ASSOCIATED CONTENT

Supporting Information

Topology and parameters for the protonated and deprotated retinal models in CHARMM format, the proton affinity as a function of C6−C7 torsion angle, the torsional energy surface for each dihedral in the polyene chain, and the coordinates of the energy minimized structures of the model compounds. This material is available free of charge via the Internet at http://pubs.acs.org.

AUTHOR INFORMATION

Corresponding Author

fellers@wabash.edu

Notes

The authors declare no competing financial interest.

ACKNOWLEDGMENTS

This work was supported by the National Science Foundation under award MCB-0950258 to S.E.F. and National Institutes of Health awards EY012049 and EY018891 to M.F.B. Computational resources were provided by NSF-MRI award CHE-1039925 through the Midwest Undergraduate Computational Chemistry Consortium. We thank R. S. Glass for discussions and N. Leioatts for assistance in preparing Figure 6.

REFERENCES

(1) Sabehi, G.; Loy, A.; Jung, K.-H.; Partha, R.; Spudich, J. L.; Isaacson, T.; Hirschberg, J.; Wagner, M. L.; Béjà, O. *PLoS Biol.* **2005**, *3*, 1409.
(2) Hirai, T.; Subramaniam, S.; Lanyi, J. K. *Curr. Opin. Struct. Biol.* **2009**, *19*, 433.
(3) Ridge, K. D.; Palczewski, K. *J. Biol. Chem.* **2007**, *282*, 9297.
(4) Hofmann, K. P.; Scheerer, P.; Hildebrand, P. W.; Choe, H.-W.; Park, J. H.; Heck, M.; Ernst, O. P. *Trends Biochem. Sci.* **2009**, *34*, 540.
(5) Smith, S. O. *Ann. Rev. Biophys.* **2010**, *39*, 309.
(6) von Lintig, J.; Kiser, P. D.; Golczak, M.; Palczewski, K. *Trends Biochem. Sci.* **2010**, *35*, 400.
(7) Smith, S. O. *Biochem. Soc. Trans.* **2012**, *40*, 389.
(8) Drews, J. *Science* **2000**, *287*, 1960.
(9) Hopkins, A. L.; Groom, C. R. *Nat. Rev. Drug Discovery* **2002**, *1*, 727.
(10) Overington, J. P.; Al-Lazikani, B.; Hopkins, A. L. *Nat. Rev. Drug Discovery* **2006**, *5*, 993.
(11) Kobilka, B.; Schertler, G. F. X. *Trends Pharmacol. Sci.* **2008**, *29*, 79.
(12) Nygaard, R.; Frimurer, T. M.; Holst, B.; Rosenkilde, M. M.; Schwartz, T. W. *Trends Pharmacol. Sci.* **2009**, *30*, 249.
(13) Ahuja, S.; Smith, S. O. *Trends Pharmacol. Sci.* **2009**, *30*, 494.
(14) Choe, H.-W.; Park, J. H.; Kim, Y. J.; Ernst, O. P. *Neuropharmacology* **2011**, *60*, 52.
(15) Katritch, V.; Cherezov, V.; Stevens, R. C. *Trends Pharmacol. Sci.* **2012**, *33*, 17.
(16) Okada, T.; Sugihara, M.; Bondar, A.-N.; Elstner, M.; Entel, P.; Buss, V. *J. Mol. Biol.* **2004**, *342*, 571.
(17) Li, J.; Edwards, P. C.; Burghammer, M.; Villa, C.; Schertler, G. F. X. *J. Mol. Biol.* **2004**, *343*, 1409.
(18) Choe, H.-W.; Kim, Y. J.; Park, J. H.; Morizumi, T.; Pai, E. F.; Kraub, N.; Hofmann, K. P.; Scheerer, P.; Ernst, O. P. *Nature* **2011**, *471*, 651.
(19) Standfuss, J.; Edwards, P. C.; D'Antona, A.; Fransen, M. R.; Xie, G.; Oprian, D. D.; Schertler, G. F. X. *Nature* **2011**, *471*, 656.
(20) Park, J. H.; Scheerer, P.; Hofmann, K. P.; Choe, H.-W.; Ernst, O. P. *Nature* **2008**, *454*, 183.
(21) Altenbach, C.; Kusnetzow, A. K.; Ernst, O. P.; Hofmann, K. P.; Hubbell, W. L. *Proc. Natl. Acad. Sci. U.S.A.* **2008**, *105*, 7439.
(22) Mahalingam, M.; Martínez-Mayorga, K.; Brown, M. F.; Vogel, R. *Proc. Natl. Acad. Sci. U.S.A.* **2008**, *105*, 17795.
(23) Ahuja, S.; Crocker, E.; Eilers, M.; Hornak, V.; Hirshfeld, A.; Ziliox, M.; Syrett, N.; Reeves, P. J.; Khorana, H. G.; Sheves, M.; Smith, S. O. *J. Biol. Chem.* **2009**, *284*, 10190.
(24) Ahuja, S.; Eilers, M.; Hirshfeld, A.; Yan, E. C. Y.; Ziliox, M.; Sakmar, T. P.; Sheves, M.; Smith, S. O. *J. Am. Chem. Soc.* **2009**, *131*, 15160.
(25) Brown, M. F.; Martínez-Mayorga, K.; Nakanishi, K.; Salgado, G. F. J.; Struts, A. V. *Photochem. Photobiol.* **2009**, *85*, 442.
(26) Zaitseva, E.; Brown, M. F.; Vogel, R. *J. Am. Chem. Soc.* **2010**, *132*, 4815.
(27) Alexiev, U.; Rimke, I.; Pohlmann, T. *J. Mol. Biol.* **2003**, *328*, 705.
(28) Brown, M. F.; Salgado, G. F. J.; Struts, A. V. *Biochim. Biophys. Acta* **2010**, *1798*, 177.
(29) Struts, A. V.; Salgado, G. F. J.; Brown, M. F. *Proc. Natl. Acad. Sci. U.S.A.* **2011**, *108*, 8263.
(30) Kirchberg, K.; Kim, T.-Y.; Möller, M.; Skegro, D.; Raju, G. D.; Granzin, J.; Büldt, G.; Schlesinger, R.; Alexiev, U. *Proc. Natl. Acad. Sci. U.S.A.* **2011**, *108*, 18690.
(31) Mertz, B.; Struts, A. V.; Feller, S. E.; Brown, M. F. *Biochim. Biophys. Acta* **2012**, *1818*, 241.
(32) Wang, Q.; Schoenlein, R. W.; Peteanu, L. A.; Mathies, R. A.; Shank, C. V. *Science* **1994**, *266*, 422.
(33) Kukura, P.; McCamant, D. W.; Yoon, S.; Wandschneider, D. B.; Mathies, R. A. *Science* **2005**, *310*, 1006.

(34) Polli, D.; Altoè, P.; Weingart, O.; Spillane, K. M.; Manzoni, C.; Brida, D.; Tomasello, G.; Orlandi, G.; Kukura, P.; Mathies, R. A.; Garavelli, M.; Cerullo, G. *Nature* **2010**, *467*, 440.
(35) Knierim, B.; Hofmann, K. P.; Ernst, O. P.; Hubbell, W. L. *Proc. Natl. Acad. Sci. U.S.A.* **2007**, *104*, 20290.
(36) Terstegen, F.; Buss, V. *Chem. Lett.* **1996**, *25*, 449.
(37) Andruniów, T.; Ferré, N.; Olivucci, M. *Proc. Natl. Acad. Sci. U.S.A.* **2004**, *101*, 17908.
(38) Frutos, L. M.; Andruniów, T.; Santoro, F.; Ferré, N.; Olivucci, M. *Proc. Natl. Acad. Sci. U.S.A.* **2007**, *104*, 7764.
(39) Sekharan, S.; Buss, V. *J. Am. Chem. Soc.* **2008**, *130*, 17220.
(40) Schapiro, I.; Weingart, O.; Buss, V. *J. Am. Chem. Soc.* **2009**, *131*, 16.
(41) Schapiro, I.; Ryazantsev, M. N.; Frutos, L. M.; Ferre, N.; Lindh, R.; Olivucci, M. *J. Am. Chem. Soc.* **2011**, *133*, 3354.
(42) Saam, J.; Tajkhorshid, E.; Hayashi, S.; Schulten, K. *Biophys. J.* **2002**, *83*, 3097.
(43) Crozier, P. S.; Stevens, M. J.; Forrest, L. R.; Woolf, T. B. *J. Mol. Biol.* **2003**, *333*, 493.
(44) Huber, T.; Botelho, A. V.; Beyer, K.; Brown, M. F. *Biophys. J.* **2004**, *86*, 2078.
(45) Phillips, J. C.; Braun, R.; Wang, W.; Gumbart, J.; Tajkhorshid, E.; Villa, E.; Chipot, C.; Skeel, R. D.; Kale, L.; Schulten, K. *J. Comput. Chem.* **2005**, *26*, 1781.
(46) Gumbart, J.; Wang, Y.; Aksimentiev, A.; Tajkhorshid, E.; Schulten, K. *Curr. Opin. Struct. Biol.* **2005**, *15*, 423.
(47) Grossfield, A.; Feller, S. E.; Pitman, M. C. *Proc. Natl. Acad. Sci. U.S.A.* **2006**, *103*, 4888.
(48) Kholmurodov, K. T.; Feldman, T. B.; Ostrovsky, M. A. *Mendeleev Commun.* **2006**, 1.
(49) Cordomi, A.; Perez, J. J. *J. Phys. Chem. B* **2007**, *111*, 7052.
(50) Grossfield, A.; Pitman, M. C.; Feller, S. E.; Soubias, O.; Gawrisch, K. *J. Mol. Biol.* **2008**, *381*, 478.
(51) Isin, B.; Schulten, K.; Tajkhorshid, E.; Bahar, I. *Biophys. J.* **2008**, *95*, 789.
(52) Neri, M.; Vanni, S.; Tavernelli, I.; Rothlisberger, U. *Biochemistry* **2010**, *49*, 4827.
(53) Hu, J.; Griffin, R. G.; Herzfeld, J. *Proc. Natl. Acad. Sci. U.S.A.* **1994**, *91*, 8880.
(54) McDermott, A. E.; Creuzet, F.; Gebhard, R.; van der Hoef, K.; Levitt, M. H.; Herzfeld, J.; Lugtenberg, J.; Griffin, R. G. *Biochemistry* **1994**, *33*, 6129.
(55) Tajkhorshid, E.; Baudry, J.; Schulten, K.; Suhai, S. *Biophys. J.* **2000**, *78*, 683.
(56) Mak-Jurkauskas, M. L.; Bajaj, V. S.; Hornstein, M. K.; Belenky, M.; Griffin, R. G.; Herzfeld, J. *Proc. Natl. Acad. Sci. U.S.A.* **2008**, *105*, 883.
(57) Palczewski, K.; Kumasaka, T.; Hori, T.; Behnke, C. A.; Motoshima, H.; Fox, B. A.; Le Trong, I.; Teller, D. C.; Okada, T.; Stenkamp, R. E.; Yamamoto, M.; Miyano, M. *Science* **2000**, *289*, 739.
(58) Martínez-Mayorga, K.; Pitman, M. C.; Grossfield, A.; Feller, S. E.; Brown, M. F. *J. Am. Chem. Soc.* **2006**, *128*, 16502.
(59) Lau, P.-W.; Grossfield, A.; Feller, S. E.; Pitman, M. C.; Brown, M. F. *J. Mol. Biol.* **2007**, *372*, 906.
(60) Hornak, V.; Ahuja, S.; Eilers, M.; Goncalves, J. A.; Sheves, M.; Reeves, P. J.; Smith, S. O. *J. Mol. Biol.* **2010**, *396*, 510.
(61) Ayton, G. S.; McWhirter, J. L.; Voth, G. A. *J. Chem. Phys.* **2006**, 124.
(62) Marrink, S. J.; Risselada, H. J.; Yefimov, S.; Tieleman, D. P.; de Vries, A. H. *J. Phys. Chem. B* **2007**, *111*, 7812.
(63) Periole, X.; Huber, T.; Marrink, S. J.; Sakmar, T. P. *J. Am. Chem. Soc.* **2007**, *129*, 10126.
(64) Brown, F. L. H. *Annu. Rev. Phys. Chem.* **2008**, *59*, 685.
(65) de Meyer, F. J. M.; Venturoli, M.; Smit, B. *Biophys. J.* **2008**, *95*, 1851.
(66) Ayton, G. S.; Voth, G. A. *J. Phys. Chem. B* **2009**, *113*, 4413.
(67) de Meyer, F. J. M.; Rodgers, J. M.; Willems, T. F.; Smit, B. *Biophys. J.* **2010**, *99*, 3629.
(68) Jensen, M. O.; Jogini, V.; Borhani, D. W.; Leffler, A. E.; Dror, R. O.; Shaw, D. E. *Science* **2012**, *336*, 229.
(69) Rasmussen, S. G. F.; Choi, H.-J.; Fung, J. J.; Pardon, E.; Casarosa, P.; Chae, P. S.; DeVree, B. T.; Rosenbaum, D. M.; Thian, F. S.; Kobilka, T. S.; Schnapp, A.; Konetzki, I.; Sunahara, R. K.; Gellman, S. H.; Pautsch, A.; Steyaert, J.; Weis, W. I.; Kobilka, B. K. *Nature* **2011**, *469*, 175.
(70) Struts, A. V.; Salgado, G. F. J.; Martínez-Mayorga, K.; Brown, M. F. *Nat. Struct. Mol. Biol.* **2011**, *18*, 392.
(71) Mertz, B.; Lu, M.; Brown, M. F.; Feller, S. E. *Biophys. J.* **2011**, *101*, L17.
(72) Tajkhorshid, E.; Paizs, B.; Suhai, S. *J. Phys. Chem. B* **1997**, *101*, 8021.
(73) Tajkhorshid, E.; Paizs, B.; Suhai, S. *J. Phys. Chem. B* **1999**, *103*, 4518.
(74) Tajkhorshid, E.; Suhai, S. *J. Phys. Chem. B* **1999**, *103*, 5581.
(75) Feller, S. E.; Gawrisch, K.; MacKerell, A. D., Jr. *J. Am. Chem. Soc.* **2002**, *124*, 318.
(76) Brooks, B. R.; Bruccoleri, R. E.; Olafson, B. D.; Swaminathan, S.; Karplus, M. *J. Comput. Chem.* **1983**, *4*, 187.
(77) Vanommeslaeghe, K.; Hatcher, E.; Acharya, C.; Kundu, S.; Zhong, S.; Shim, J.; Darian, E.; Guvench, O.; Lopes, P.; Vorobyov, I.; MacKerell, A. D., Jr. *J. Comput. Chem.* **2010**, *31*, 671.
(78) Nina, M.; Roux, B.; Smith, J. C. *Biophys. J.* **1995**, *68*, 25.
(79) Liptak, M. D.; Shields, G. C. *J. Am. Chem. Soc.* **2001**, *123*, 7314.
(80) Chamberlin, A. C.; Cramer, C. J.; Truhlar, D. G. *J. Phys. Chem. B* **2008**, *112*, 8651.
(81) Sheves, M.; Albeck, A.; Friedman, N.; Ottolenghi, M. *Proc. Natl. Acad. Sci. U.S.A.* **1986**, *83*, 3262.
(82) Martinez-Mayorga, K.; Pitman, M. C.; Grossfield, A.; Feller, S. E.; Brown, M. F. *J. Am. Chem. Soc.* **2006**, *128*, 16502.
(83) Cherezov, V.; Rosenbaum, D. M.; Hanson, M. A.; Rasmussen, S. G. F.; Thian, F. S.; Kobilka, T. S.; Choi, H.-J.; Kuhn, P.; Weis, W. I.; Kobilka, B. K.; Stevens, R. C. *Science* **2007**, *318*, 1258.
(84) Rasmussen, S. G. F.; Choi, H.-J.; Rosenbaum, D. M.; Kobilka, T. S.; Thian, F. S.; Edwards, P. C.; Burghammer, M.; Ratnala, V. R. P.; Sanishvili, R.; Fischetti, R. F.; Schertler, G. F. X.; Weis, W. I.; Kobilka, B. K. *Nature* **2007**, *450*, 383.
(85) Jaakola, V.-P.; Griffith, M. T.; Hanson, M. A.; Cherezov, V.; Chien, E. Y. T.; Lane, J. R.; IJzerman, A. P.; Stevens, R. C. *Science* **2008**, *322*, 1211.
(86) Rosenbaum, D. M.; Zhang, C.; Lyons, J. A.; Holl, R.; Aragao, D.; Arlow, D. H.; Rasmussen, S. G. F.; Choi, H.-J.; DeVree, B. T.; Sunahara, R. K.; Chae, P. S.; Gellman, S. H.; Dror, R. O.; Shaw, D. E.; Weis, W. I.; Caffrey, M.; Gmeiner, P.; Kobilka, B. K. *Nature* **2011**, *469*, 236.
(87) Cai, M.; Nyberg, J.; Hruby, V. J. *Curr. Top. Med. Chem.* **2009**, *9*, 554.
(88) Vagner, J.; Xu, L.; Handl, H. L.; Josan, J. S.; Morse, D. L.; Mash, E. A.; Gillies, R. J.; Hruby, V. J. *Angew. Chem., Int. Ed.* **2008**, *47*, 1685.
(89) Brown, M. F. *Curr. Top. Membranes* **1997**, *44*, 285.
(90) Farrens, D. L.; Altenbach, C.; Yang, K.; Hubbell, W. L.; Khorana, H. G. *Science* **1996**, *274*, 768.
(91) Herzfeld, J.; Tounge, B. *Biochim. Biophys. Acta-Bioenerg.* **2000**, *1460*, 95.
(92) Eikhom, T. S.; Jonsen, J.; Laland, S.; Refsvik, T. *Biochem. Biophys. Acta* **1963**, *76*, 465.
(93) Botelho, A. V.; Huber, T.; Sakmar, T. P.; Brown, M. F. *Biophys. J.* **2006**, *91*, 4464.
(94) Grossfield, A.; Pitman, M. C.; Feller, S. E.; Soubias, O.; Gawrisch, K. *J. Mol. Biol.* **2008**, *381*, 478.
(95) Nakamichi, H.; Okada, T. *Proc. Natl. Acad. Sci. U.S.A.* **2006**, *103*, 12729.
(96) Nakamichi, H.; Okada, T. *Angew. Chem., Int. Ed.* **2006**, *45*, 4270.
(97) Sharma, A. K.; Spudich, J. L.; Doolittle, W. F. *Trends Microbiol.* **2006**, *14*, 463.